Hindawi
Wireless Communications and Mobile Computing
Volume 2022, Article ID 9906100, 12 pages
https://doi.org/10.1155/2022/9906100

Research Article

Research on Reconfiguration of Distribution Network considering Three-Phase Unbalance

Xuejie Wang[1,2] **Yanchao Ji**[1] **Jianze Wang**[1] **Yi Zhao**[2] **Peng Ye**[2] **Lei Qi**[3] **Shuo Yang**[4] **and Siqi Liu**[4]

[1]*School of Electrical Engineering &Automation, Harbin Institute of Technology, Harbin 150001, China*
[2]*School of Electric Power, Shenyang Institute of Engineering, Shenyang 110136, China*
[3]*Liaoning Provincial Institute of Safety Science, 110004 Shenyang, China*
[4]*Fushun Power Supply Company, State Grid Liaoning Electric Power Supply Co Ltd, Fushun 113008, China*

Correspondence should be addressed to Xuejie Wang; wangxj1@sie.edu.cn

Received 16 April 2022; Revised 21 June 2022; Accepted 6 July 2022; Published 18 August 2022

Academic Editor: Jun Ye

Copyright © 2022 Xuejie Wang et al. This is an open access article distributed under the Creative Commons Attribution License, which permits unrestricted use, distribution, and reproduction in any medium, provided the original work is properly cited.

In the distribution network, the addition of distributed power sources can improve the voltage part of the distribution system, provide uninterrupted power supply, and reduce network losses. The location of the power supply and its output will also directly affect the system voltage and power loss. Therefore, determining the optimal installation location and capacity of distributed power generation is of great significance to the distribution network. However, in the actual system, due to the unbalanced load distribution and the three-phase unbalance of the transmission line, the power distribution system presents the characteristics of unbalanced distribution. As the number of electric vehicles increasing, the imbalance of the distribution network has become more prominent.

1. Introduction

Distribution network reconfiguration is of great significance to the planning and operation of the distribution network. Reconfiguration can determine the topology of the network to improve the economy and stability of the operation of the system. Distributed power has aggravated the three-phase imbalance of system. The goal of the reconfiguration program is to determine the optimal network topology path by controlling the switch state, to meet the system's minimum network loss and load balance objective function, and to some given distribution network operation constraints [1, 2]. Due to the nonlinearity of power flow and the discreteness of switching states, the problem of distribution network reconstruction can be regarded as a mixed integer nonlinear problem in mathematics. In the previous theoretical research, heuristic algorithms have been studied in depth [3, 4]. In addition, many global optimization algorithms are applied, such as genetic algorithm [5], artificial neural networks [6], and particle swarm optimization [7]. The calculations of these methods are usually more complicated, and they cannot guarantee the global optimal solution. In mathematical optimization problems, reconstruction models are usually expressed as linear programming problems [8], quadratic programming problems [9], etc. Although a lot of results have been obtained in the algorithm for solving the reconstruction problem, most of the existing algorithms are obtained under the assumption that the distribution network is a three-phase balanced system. In the actual system, due to the unbalanced load and network structure, the distribution network operates in a three-phase unbalanced state. In order to solve the above imbalance problem, the literature [10] proposed a real-time distribution network reconstruction algorithm for three-phase unbalanced systems.

2. Three-Phase Unbalanced System Model

In a three-phase unbalanced power distribution system, the relationship between voltage and current can be expressed in Figure 1.

$$\begin{bmatrix} \boldsymbol{V}_i^a \\ \boldsymbol{V}_i^b \\ \boldsymbol{V}_i^c \end{bmatrix} = \begin{bmatrix} \boldsymbol{V}_j^a \\ \boldsymbol{V}_j^b \\ \boldsymbol{V}_j^c \end{bmatrix} + \begin{bmatrix} z_{aa} & z_{ab} & z_{ac} \\ z_{ba} & z_{bb} & z_{bc} \\ z_{ca} & z_{cb} & z_{cc} \end{bmatrix} \cdot \begin{bmatrix} \boldsymbol{I}_i^a \\ \boldsymbol{I}_i^b \\ \boldsymbol{I}_i^c \end{bmatrix}. \tag{1}$$

The load model can be regarded as a negative sequence injection current in the system, and each load is assumed to be a constant power component, a linear combination of a constant impedance component, and a constant current component. Therefore, the three-phase injection current at the i bus can be expressed as

$$[\boldsymbol{I}_{L,i}]_{abc} = \alpha_{1,i} \cdot [\boldsymbol{I}_{\mathrm{P},i}]_{abc} + \alpha_{2,i} \cdot [\boldsymbol{I}_{\mathrm{Z},i}]_{abc} + \alpha_{3,i} \cdot [\boldsymbol{I}_{\mathrm{I},i}]_{abc}, \tag{2}$$

where $[\boldsymbol{I}_{P,i}]_{abc}$ is the constant power three-phase injection current component; $[\boldsymbol{I}_{\mathrm{Z},i}]_{abc}$ is the constant impedance three-phase injection current component; and $[\boldsymbol{I}_{\mathrm{I},i}]_{abc}$ is the three-phase injection current component of constant current.

The distributed power model at the i bus can be regarded as the positive sequence injection current as

$$[I_{\mathrm{DG},i}]_{abc} = \left[\frac{P^{\mathrm{a}}_{\mathrm{DG},i} - jQ^{\mathrm{a}}_{\mathrm{DG},i}}{V_{\mathrm{i}}^{a^*}} \quad \frac{P^{\mathrm{b}}_{\mathrm{DG},i} - jQ^{b}_{\mathrm{DG},i}}{V_{\mathrm{i}}^{b^*}} \quad \frac{P^{c}_{\mathrm{DG},i} - jQ^{c}_{\mathrm{DG},i}}{V_{\mathrm{i}}^{c^*}} \right]^T, \tag{3}$$

where $P^{\mathrm{a}}_{\mathrm{DG},i}$, $P^{\mathrm{b}}_{\mathrm{DG},i}$, and $P^{c}_{\mathrm{DG},i}$ are, respectively, the three-phase active power of the distributed power supply at bus i and $Q^{\mathrm{a}}_{\mathrm{DG},i}$, $Q^{b}_{\mathrm{DG},i}$, and $Q^{c}_{\mathrm{DG},i}$ are, respectively, the three-phase reactive power of the distributed power supply at bus i.

When the distributed power supply operates in constant power operation mode, the equivalent injection current can be directly derived from Equation (3). When the distributed power supply operates in constant voltage mode, a double-loop calculation is required to obtain the equivalent injection current. The inner-loop calculation yields the amount of distributed power supply reactive power required to keep the bus voltage in a fixed range. The outer-loop calculation can obtain the injection current from the initial active power and the calculated reactive power. In a three-phase asymmetric system with two-phase or single-phase branches, the impedance of the missing phase in Equation (1) is zero, and the voltage and current of the missing phase can be excluded from the calculation results. Correspondingly, the current values of the missing phases in Equations (2) and (3) can be set to zero.

Distribution network reconfiguration is generally viewed as feeder reconfiguration optimization problem, and it is usually assumed that only three-phase feeder branches are available for reconfiguration. Any line is equipped with three-phase switching equipment, and the switch states can be defined as

$$S_j = \begin{cases} 1, \text{Switch j is closed, consistent with the initial direction} \\ 0, \text{Switch j is off} \\ -1, \text{Switch j is closed, opposite to the initial direction} \end{cases}, \tag{4}$$

where the direction of reference is determined by the direction of current.

The network connectivity of the distribution network is characterized by the node-branch correlation matrix. If the system is an ideal three-phase symmetric system, a single-phase equivalent circuit is usually adopted, as well as the node-branch correlation matrix $\boldsymbol{A}_{balanced}$ determined by the structure of system. The initial test state of the distribution network assumes that the switches are all closed. The initial node-branch correlation matrix A_0 of the network is symmetric, and A_0 is constant for a given network.

where a_{ij}^0 is the matrix elements of $\boldsymbol{A}_0$.

If the distribution network is a three-phase asymmetric system, the node-branch correlation matrix is three-phase and is obtained by multiplying $\boldsymbol{A}_{balanced}$ by a unit matrix of order 3:

$$A(i,j) = \begin{bmatrix} a_{ij} & 0 & 0 \\ 0 & a_{ij} & 0 \\ 0 & 0 & a_{ij} \end{bmatrix} = \begin{bmatrix} a_{ij}^0 & 0 & 0 \\ 0 & a_{ij}^0 & 0 \\ 0 & 0 & a_{ij}^0 \end{bmatrix} \cdot S_{\mathrm{j}}. \tag{5}$$

And

$$\boldsymbol{I}_{bus} = \left(\boldsymbol{A} \cdot \boldsymbol{Y}_{branch} \cdot \boldsymbol{A}^T\right) \cdot \boldsymbol{V}_{\mathrm{bus}} = \boldsymbol{Y}_{\mathrm{bus}} \cdot \boldsymbol{V}_{\mathrm{bus}}. \tag{6}$$

Among them,

Where $\boldsymbol{I}_{bus}$ is the node injection current vector; $\boldsymbol{V}_{\mathrm{bus}}$ is the bus voltage vector; $\boldsymbol{Y}_{\mathrm{bus}}$ is the nodal conductivity matrix; and $\boldsymbol{Y}_{branch}$ is the tributary conductivity matrix.

$$\boldsymbol{I}_{bus} = \boldsymbol{I}_{DG} - \boldsymbol{I}_L, \tag{7}$$

where $\boldsymbol{I}_{DG}$ is the distributed power injection current vector and $\boldsymbol{I}_L$ is the load injection current vector.

According to Equations (6) and (7), the tidal current calculation can be expressed as follows: the initial voltage $\boldsymbol{V}_{\mathrm{bus}}^{k-1}$ is given, the nodal injection current $\boldsymbol{I}_{\mathrm{bus}}^{k}$ can be solved by Equation (7), and $\boldsymbol{V}_{\mathrm{bus}}^{k}$ is calculated by substituting $\boldsymbol{I}_{\mathrm{bus}}^{k}$ into Equation (6). When the termination condition is satisfied, the iterative termination calculation in turn leads to the system nodal voltage and branch current values.

Equation (7) can in turn be expressed as

$$\boldsymbol{I}_{\mathrm{bus},i}^{l} = \sum_{k=1}^{n} \sum_{p=a}^{c} t_{ik}^{lp} \cdot v_k^p, l = phase\ a, b, c. \tag{8}$$

In the formula, $t_{ik}^{lp} = \sum_{j=1}^{m} (a_{ij}^0 a_{kj}^0 y_j^{lp}) \cdot S_j^2 \triangleq g_{ik}^{lp} + j b_{ik}^{lp}$.

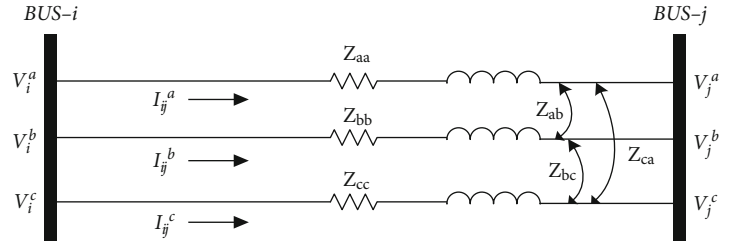

Figure 1: Improved hierarchical decentralized reconstruction method process.

$[y_j^{aa}, y_j^{ab}, y_j^{ac}; y_j^{ba}, y_j^{bb}, y_j^{bc}; y_j^{ca}, y_j^{cb}, y_j^{cc}]$ is the conjugate inverse matrix of the jth branch impedance matrix. Due to the existence of the relation of Equation (9):

$$\boldsymbol{I}_{bus,i}^{l} = \frac{P_{inject,i}^{l} - j \cdot Q_{inject,i}^{l}}{e_i^l - j \cdot f_i^l}, \tag{9}$$

where $P_{inject,i}^{l}, Q_{inject,i}^{l}$ is the active and reactive injected power at node i of a phase.

The tide calculation formula can be obtained as

$$\begin{cases} P_{inject,i}^{l} = \sum_{k=1}^{n} \sum_{p=a}^{c} \left\{ e_i^l \left(g_{ik}^{lp} \cdot e_k^p - b_{ik}^{lp} \cdot f_k^p \right) + f_i^l \left(g_{ik}^{lp} \cdot f_k^p - b_{ik}^{lp} \cdot e_k^p \right) \right\} \\ Q_{inject,i}^{l} = \sum_{k=1}^{n} \sum_{p=a}^{c} \left\{ f_i^l \left(g_{ik}^{lp} \cdot e_k^p - b_{ik}^{lp} \cdot f_k^p \right) - e_i^l \left(g_{ik}^{lp} \cdot f_k^p + b_{ik}^{lp} \cdot e_k^p \right) \right\} \end{cases}. \tag{10}$$

In power loss, in an unbalanced system, the result of power loss in the branch is the input power minus the output power of each phase, so we can obtain

$$A^T \cdot V_{bus} = Z_{branch} \cdot I_{branch}. \tag{11}$$

Substituting Equations (1) and (5) into Equation (11), the total active power loss can be obtained as

$$\begin{aligned} P_{loss} &= \mathrm{Re} \left\{ \sum_{j=1}^{n} \left[\sum_{k=a}^{c} \left(V_j^{k^*} \cdot \sum_{i=1}^{n} \left(\sum_{p=a}^{c} V_i^p \cdot \left(\sum_{i=1}^{m} a_{il}^0 a_{jl}^0 y_l^{pk} \cdot s_l^2 \right) \right) \right) \right] \right\} \\ &= \sum_{j=1}^{n} \sum_{k=a}^{c} \sum_{i=1}^{n} \sum_{p=a}^{c} \left\{ e_j^k \cdot \left(e_i^p \cdot g_{ij}^{pk} + f_i^p \cdot b_{ij}^{pk} \right) \right. \\ &\quad \left. + f_j^k \cdot \left(f_i^p \cdot g_{ij}^{pk} - e_i^p \cdot b_{ij}^{pk} \right) \right\}. \end{aligned} \tag{12}$$

The magnitude of the voltage depends on the network topology of the system and the output power of the distributed power supply, which are the two variables that satisfy the power loss minimization objective function. In addition to this, the operational constraints have to be satisfied:

2.1. Voltage Amplitude Constraint.

$$V_{imin} \le |V_i^a|, \left| V_i^b \right|, |V_i^c| \le V_{imax}, i = 1, 2, \cdots, N, \tag{13}$$

where V_{imin} and V_{imax} are the allowable minimum and maximum voltages of node i, respectively, so that V_{imin} is 0.95 times the rated voltage and V_{imax} is 1.05 times the rated voltage.

2.2. Node Voltage Imbalance Constraint. Voltage imbalance can be obtained by dividing the maximum voltage deviation by the average voltage amplitude of the three phases. According to ANSI C84.1-2011, the voltage imbalance should be controlled within 3%. Therefore, the voltage imbalance constraint can be expressed as

$$\left| \frac{\left| V_i^p \right| - avg_i}{avg_i} \right| \le 3\%, \text{ where, } avg_i = \sum_{p=a}^{c} \left| V_i^p \right| / 3, p = a, b, c. \tag{14}$$

2.3. Current Constraint.

$$\left| I_{branch,i}^{p} \right| \le I_{\mathrm{i,max}}, \tag{15}$$

where $I_{\mathrm{i,max}}$ is the load capacity of branch i.

2.4. Network Radiation-like Structural Constraints. Network constraints and balanced systems are systems where the distribution network remains radial in operation. The network of unbalanced system is radial network.

$$\sum_{k=1}^{M} |S_k| = N - d, \tag{16}$$

where d is the number of all balancing nodes.

All loads are supplied with uninterrupted power supply, rank $(A) = N - d$. At least one branch in each loop is open and closed.

$$\sum_{i=1}^{M_k} |S_i| \le M_k - 1, \tag{17}$$

where M_k is the number of branches of loop k.

3. Optimal Planning of DG Units

According to the literature [11], the results show that the factors affecting the system power loss include the network topology, the location, and the output power of DG units. The sensitivity of the injected active power loss per bus can

be used to determine the optimal bus location for installing the distributed power units.

3.1. DG Optimal Location of the Unit. Since the integration of distributed power units increases the bus active power injection, the best installation location is the bus with the maximum negative active loss sensitivity [12] so that power loss will be effectively controlled. Define the power loss Equation (13) as

$$P_{loss} = g(e, f). \tag{18}$$

The relationship between the voltage vector and the injected power is determined from Equation (10):

$$h\left(e, f, P_{inject}, Q_{inject}\right) = 0. \tag{19}$$

If the small variation $[\Delta P, \Delta Q]^T$ is added to the injected power vector $[P_{inject}, Q_{inject}]^T$, the variation of the voltage vector can be solved by Equation (15):

$$\left[\frac{\partial h}{\partial e} \quad \frac{\partial h}{\partial f}\right]\Bigg|_{x^0} \cdot \begin{bmatrix} \triangle e \\ \Delta f \end{bmatrix} + \left[\frac{\partial h}{\partial P_{inject}} \quad \frac{\partial h}{\partial Q_{inject}}\right]\Bigg|_{x^0} \cdot \begin{bmatrix} \triangle P_{inject} \\ \Delta Q_{inject} \end{bmatrix} = 0. \tag{20}$$

Therefore, the amount of change in power loss caused is shown in Equation (21):

$$\triangle P_{loss} = \left[\frac{\partial g}{\partial e} \quad \frac{\partial g}{\partial f}\right] \cdot \begin{bmatrix} \triangle e \\ \triangle f \end{bmatrix}. \tag{21}$$

Then, the power loss sensitivity vector for each bus injected power is

$$M_s = -\left[\frac{\partial g}{\partial e} \quad \frac{\partial g}{\partial f}\right] \cdot \left(\left[\frac{\partial \mathrm{h}}{\partial e} \quad \frac{\partial h}{\partial f}\right]\right)^{-1} \cdot \left(\left[\frac{\partial \mathrm{h}}{\partial P_{inject}} \quad \frac{\partial h}{\partial Q_{inject}}\right]\right). \tag{22}$$

The sensitivity vector is solved to obtain the power loss sensitivity of the injected power of each phase of the busbar. It is considered that only the busbars of three phases can be used as candidate installation locations; then, the sensitivity of each busbar is taken as the average of the sensitivity of the three phases.

3.2. Optimal Capacity of DG Units. The optimal capacity of the DG unit minimizes the power loss in the unit in an unbalanced system that keeps the initial topology constant [13].This case can be considered an undesirable situation in reconfiguration studies, due to the fact that the DG unit needs to emit the maximum power and there is no other way to additionally support the reconfiguration. The influence of the optimal capacity of distributed generation is as follows: The optimal capacity of the DG unit is solved so that the power loss of the unit can be minimized in the unbalanced distribution system with initial topology. This scenario can be considered the worst case in reconfiguration research. Because DG units must generate maximum power into the grid, there is no need for additional support to reconfigure the network. After installing the DG unit and arranging its optimum capacity, the power loss of the system has been minimized under the initial system structure. Power optimization may be further reduced if the system is reconfigured. In addition, due to time-varying load, power losses are not always minimized in the case of a fixed network structure and constant DG output power. It is therefore necessary to reconfigure the network and reduce the DG power from time to time [14].

The optimization problem of the optimal capacity can be expressed as

$$\min_u J = P_{loss}(x, u) \quad s.t. \begin{cases} f(x, u) = 0 \\ g(x, u) \le 0 \end{cases}. \tag{23}$$

In the formula: $x = [e, f]^T$, $u = [P_{DG}, Q_{DG}]^T$, $f(x, u)$ is the tidal equation, and $\mathrm{g}(x, u)$ denotes the inequality constraint of Equations (13)–(17). The inequality constraint can be eliminated by introducing a penalty function in the objective function, and Equation (23) can be expressed as

$$\min J_{uc} = P_{loss}(x, u) + \sum_{i=1}^{H} \phi_i(\beta_i, g_i), \tag{24}$$

where H is the total number of inequality constraints.

Each penalty function is defined as

$$\phi_i(\beta_i, g_i) = \begin{cases} 0, & \text{if } g_i \le 0 \\ \beta_i, g_i^2, & \text{if } g_i > 0 \end{cases} \text{and} \beta_i > 0. \tag{25}$$

The tide calculation is first performed to obtain the power loss such that the equation constraint $f(x, u)$ is always satisfied. Thus, Equation (25) becomes an unconstrained optimization problem, and its minimum can be solved using the proposed Newtonian numerical method; the differentiation of Equation (26) is

$$\mathrm{F(u)} = \frac{dJ_{uc}(\mathrm{x}, \mathrm{u})}{du} = \frac{dP_{loss}(\mathrm{x}, \mathrm{u})}{du} + \frac{d}{d_u}\sum_{i=1}^{H} \phi_i(\beta_i, g_i). \tag{26}$$

In the formula, the first part of the rightmost side of the equation is the same as the sensitivity matrix, whose matrix columns represent the bus of the selected DG unit. The second term can be obtained by differentiating the inequality constraint. Since the second-order partial derivative

equation of the multivariate function is difficult to solve, the minimum of Equation (26) can be solved by the cutline method with positive definite cutline update.

$$\begin{aligned} u_{k+1} &= u_k - H_k^{-1} \cdot F(u_k), \\ s_k &= u_{k+1} - u_k, y_k = F(u_{k+1}) - F(u_k), \\ H_{k+1} &= H_k + \frac{y_k \cdot y_k^T}{y_k^T \cdot s_k} - \frac{H_k \cdot s_k \cdot s_k^T \cdot H_k}{s_k^T \cdot H \cdot s_k}. \end{aligned} \tag{27}$$

4. Network Reconfiguration of DG Units

After installing the DG units and adjusting their optimal capacity as described above, the system network losses are at their lowest level under the initial network topology. A network reconfiguration is required to bring the power loss down further. In addition, due to the fluctuating load, the power loss is not always minimal with a constant topology and a constant DG [15]. Therefore, in each operational interim period, the objective function is defined as minimizing the total cost of power loss and limiting the output power of the DG set. The problem is described as

$$\begin{aligned} \min J = & \left(\begin{array}{c} w_1 \cdot P_{loss}(S, PQ_{DGact}) + w_2 \sum_{i=1}^{k} \sum_{p=a}^{c} \left(P^p_{DG\ \max,i} - \left(P^p_{DGact,i} \right)_t \right) \\ + w_3 \sum_{i=1}^{k} \sum_{p=a}^{c} \left(Q^p_{DG\ \max,i} - \left(Q^p_{DGact,i} \right)_t \right) \end{array} \right) \cdot \triangle T \\ & s.t. (13) \sim (17), \text{and} \\ & \left(P^p_{DGact,i} \right)_t \le P^p_{DG\ \max,i}, \left(Q^p_{DGact,i} \right)_t \le Q^p_{DG\ \max,i}, \\ & i = 1 \sim k, p = a, b, c, t = 1 \sim 24. \end{aligned} \tag{28}$$

where T is the number of contact switches; K is the number of DG units; ΔT is the scheduled running time in hours; $P^p_{DG\ \max,i}$, $Q^p_{DG\ \max,i}$ is the optimal capacity of the i-th DG unit; and $(P^p_{DGact,i})_t$, $(Q^p_{DGact,i})_t$ is the p ($p = a,b,c$) phase active and reactive power output by the ith DG unit at time t of operation.

Since the optimization problem of distribution network reconfiguration considering three-phase imbalance is a second-order partial derivative equation solution problem for multivariate functions, therefore, an improved hierarchical decentralized reconstruction method is adopted to simultaneously reconstruct the optimal topology of the distribution network considering the three-phase imbalance and regulate the DG output power. The flowchart is shown in Figure 2:

4.1. Network Decomposition. Loops are more easily identified by the difference between closed contact switches and segmented opens for differentiation. In order to easily distinguish between tightly connected partitions and loosely connected partitions [16], the connectivity between the subdivisions is defined as follows:

$$\mathrm{D(A, B)} = \frac{\text{Number of public bus}}{\min\left(\text{Total number of busbars in zone A, Total number of busbars in zone B}\right)}, \tag{29}$$

If $\mathrm{D(A, B)} = 0$, it means that partition A and partition B are independent of each other. Given a threshold δ, if, means that partition A and partition B are tightly connected and if $\mathrm{D(A, B)} \le \delta$ means that partition A and partition B are loosely connected. However, if the threshold δ is set too small, the loosely connected partitions are not easily identified; if the threshold δ is set too large, the loosely connected partitions are easily expanded. Therefore, it is generally reasonable to choose a threshold δ of 0.2.

The specific steps of network decomposition are as follows.

The set of cut vertices of a connected graph $\mathrm{G} = (\mathrm{V}, \mathrm{E})$ is a vertex set $U \subseteq V$ satisfying the following conditions: G-U is not connected; G-K is connected, $K \subset U$; every vertex u of U in a connected graph G is connected to at least one vertex in every partition of G-U. A set of cut vertices is a cut vertex if there is only one vertex in the set.

(a) The value of the modified adjacency matrix **C** is acquired. Let $\boldsymbol{m}$ be the number of loops, and the modified adjacency matrix is an m-dimensional square matrix

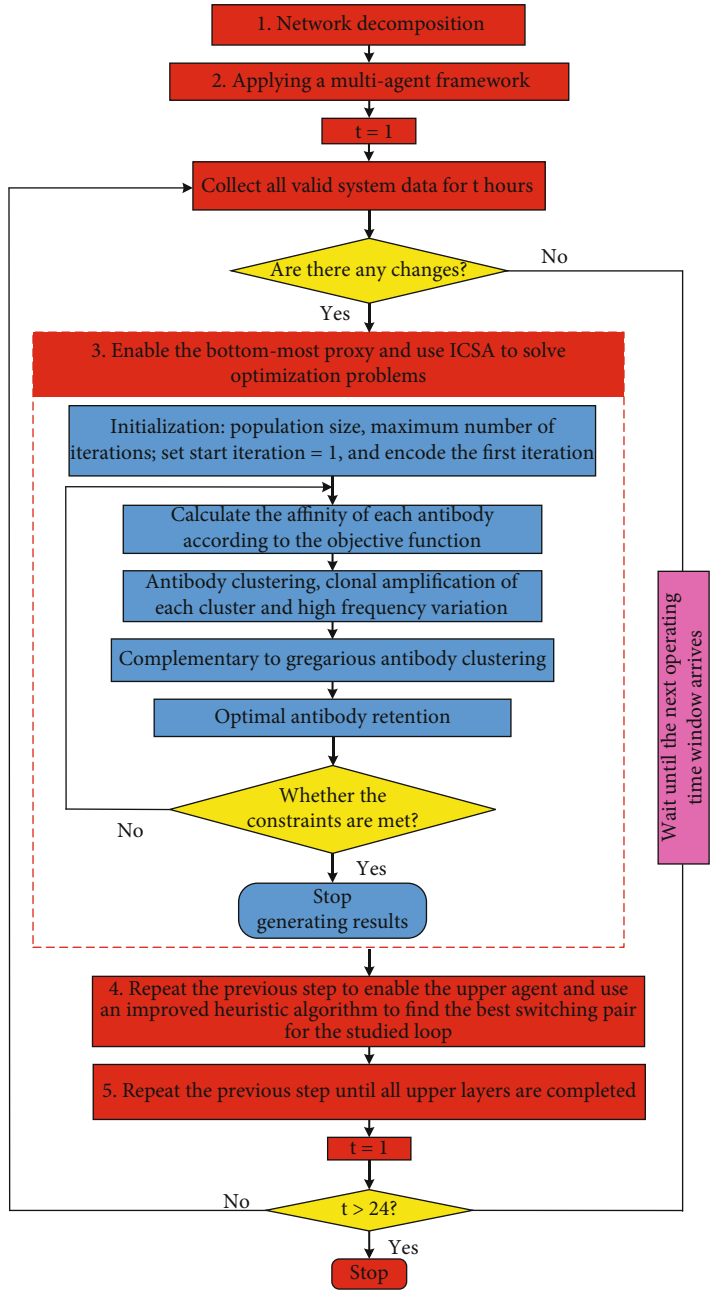

Figure 2: Improved hierarchical decentralized reconstruction method process.

(b) If there are no partitions with a common bus other than the source node, these partitions are defined as basic partitions. Two basic partitions are connected to each other by a contact switch. The following steps are used for all basic partitions

(c) Draw the connectivity graph. In the connectivity graph $G = (V, E)$, the set of vertices $V = \{v_1, \cdots, v_n\}$ represents **1 – n** loops. The edge **E** connecting the vertices indicates that the loops are coupled to each other. The vertices are drawn in the studied region to represent the loops, and if the element C (i, j) is not zero, an edge is added between the vertices v_i and v_j. If loop **i** is loosely connected to loop **j**, then it is noted as L; otherwise, it is noted as **T**

(d) Be sure to check graph G for connectivity. If not, the isolated vertices need to be found, denoted as *S*. The corresponding loop of the isolated vertex contains the first member of the decomposition system

(e) Determine the cut vertex set of G-s. The search starts from the parent node, and the cut vertex set node is found from the child nodes associated with the parent node. If the cut vertex set is empty, the search moves to the vertex associated with the child node.

Table 1: The structure of chromosomes.

OS_1-OS_T	P_{1a}	Q_{1a}	P_{1b}	Q_{1b}	P_{1c}	Q_{1c}	…	P_{Ka}	Q_{Ka}	P_{Kb}	Q_{Kb}	P_{Kc}	Q_{Kc}

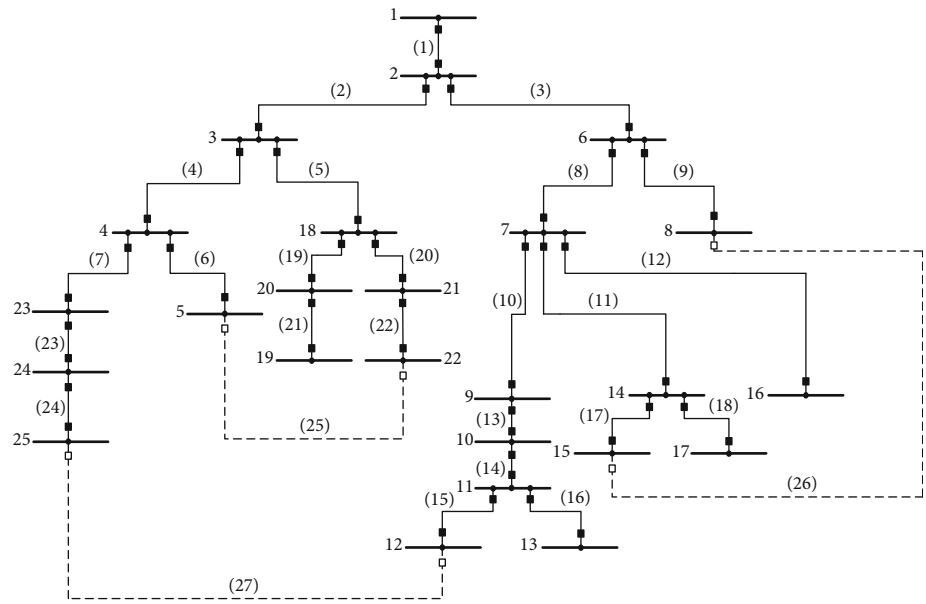

Figure 3: The single-line diagram of the 25-bus unbalanced distribution system.

Table 2: Optimal capacity of DG units for three scenarios.

Scenario	Installation site	Optimal capacity region					
		Phase A		Phase B		Phase C	
		Active (kw)	Reactive (KVar)	Active (kw)	Reactive (KVar)	Active (kw)	Reactive (KVar)
1	12	356.2	362.4	420.5	368.3	258.4	189.3
	Three − phase minimum voltage = [0.966,0.965, 0.956 pu] Power loss =224.2 kW; maximum voltage imbalance =2.236%						
2	12	220.5	158.2	210.8	172.4	214.8	165.9
	13	214.8	156.7	208.6	163.2	212.4	162.5
	Three − phase minimum voltage = [0.964,0.965,0.963 pu] Power loss = 192.8 kW; maximum voltage imbalance = 0.562%						
3	12	136.5	103.6	145.2	106.3	148.6	108.2
	13	135.2	104.5	143.8	102.6	146.3	105.8
	11	152.6	116.2	160.5	116.5	162.6	115.6
	Three − phase minimum voltage = [0.963, 0.965, 0.965 pu] Power loss = 186.2 kW; maximum voltage imbalance = 0.358%						

If the cut vertex set is found, the cut vertex set is removed, and the associated edges define two separate components. Continue searching for each component's cut vertex set until there are no more cut vertex sets. Each component represents the decomposed system, and the contact switch corresponding to the cut vertex set represents the decomposed system by the links between them

(f) In case two vertices are connected to the edge marked with ***L***, their corresponding rings are decomposed into two subsystems. If two loosely connected vertices are tightly connected to another vertex, the contact switch corresponding to that vertex is an interconnection between the two subsystems. In the lowest level subsystem forming the basis of the entire system, which includes all busbars, loads, and DG units. Each higher-level subsystem consists of several subsystems representing the entire system

4.2. Applying a Multi-Agent Framework. Intelligent agents consisting of data units, computation units, and decision units need to be assigned to each subsystem for solving subproblems of the assigned subsystem and exchanging

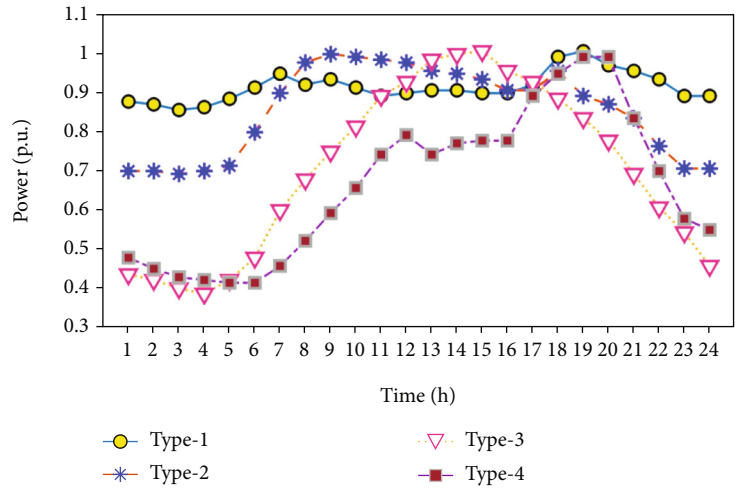

Figure 4: Four groups of load shapes.

Table 3: The optimal switching plan.

Time window	Open switches	Time window	Open switches	Time window	Open switches
0-1 h	15, 17, 22	9-10 h	15, 17, 22	17-18 h	15, 17, 22
2-3 h	15, 17, 22	10-11 h	17, 24, 6	18-19 h	15, 17, 22
3-4 h	15, 17, 22	11-12 h	15, 17, 22	19-20 h	15, 17, 22
4-5 h	15, 17, 22	12-13 h	17, 24, 22	20-21 h	15, 17, 22
5-6 h	15, 17, 22	13-14 h	15, 17, 22	21-22 h	15, 17, 22
6-7 h	15, 17, 22	14-15 h	17, 24, 22	22-23 h	17, 24, 6
7-8 h	17, 24, 6	15-16 h	17, 24, 6	23-24 h	15, 17, 22
8-9 h	15, 17, 22	16-17 h	15, 17, 22		

information with other agents. Since DG units may exist in the bottom most subsystem, the bottom most agent should be able to decide the optimal topology and the best DG output of the local system. The optimization problem for each bottom most agent layer is represented by Equation (29), and all variables are refined into local variables for its subsystem. Based on the decision plan solved by the lower layer agents, all upper layer agents ought to judge whether the common contact switch is off or not; hence, each embedded optimization problem is a pure reconstruction problem with the equation:

$$\min J = P_{loss}\left(S_{subsystem}, S_{solved}, PQ_{solved}\right) \cdot \Delta T. \quad (30)$$

In the formula, $S_{subsystem}$ is the set of switching states to be solved; S_{solved} is the set of switching states already solved by the lower layer agent; and PQ_{solved} is the actual output power of the DG unit of the lowest layer agent.

4.3. Optimization Problems for the Lowest-Level Agent. The optimization problem defined in the bottom-most agent is a mixed-integer nonlinear problem, switch states, and DG outputs selected as decision variables. The immune clonal selection differential evolution algorithm is utilized to solve the mixed integer nonlinear optimization problem defined in the bottom-most surrogate [17]. Due to the presence of DG in the decision variables, some changes have been made to the algorithm. A considerable number of antibody groups are generated from genes that determine antibodies, which are used as the initial antibody groups for the differential evolution algorithm of immune clone selection as shown in Table 1.

The definition of antibody genes is shown in Table 1, and there are T +6 K genes in total: The first T gene represents the open switch; the following 6 K genes are the active and reactive power generated by the Kth DG unit. Antibody clustering, clonal expansion, and high-frequency mutation randomly select a gene i from T +6 K genes; get high-frequency mutation to randomly change a selected gene, and introduce new information into offspring. The selected gene could represent the open switch. Before evaluating fitness values for new antibody clusters, all duplicate antibodies were removed, and the viability of each progeny was assessed by sequentially examining system structural constraints and voltage/current constraints. Then, the fitness values of all viable progeny are calculated, and the best antibody is selected. Finally, the optimal topology of all the lowest-level subsystems and the optimal output of the DG unit are solved. The agents coordinate when necessary, passing the final result to the upper agent to activate the computation. The network reconstruction problem is solved separately and decomposed into different subproblems. A hierarchical structure is used to assign independent agents to subproblems to realize parallel computing. Each agent is made up of three units. The data unit collects local information and communicates with other agents. The computational unit realizes the improved heuristic algorithm to solve the local reconstruction problem, and the decision unit completes the coordination control. The calculation result of the lower agent is transmitted to the data unit of the upper agent. The final optimal configuration is completed by the collaboration between multiple agents.

4.4. Upper Layer Proxy Startup Issues. A heuristic algorithm based on branch-and-switch and single-loop optimization is

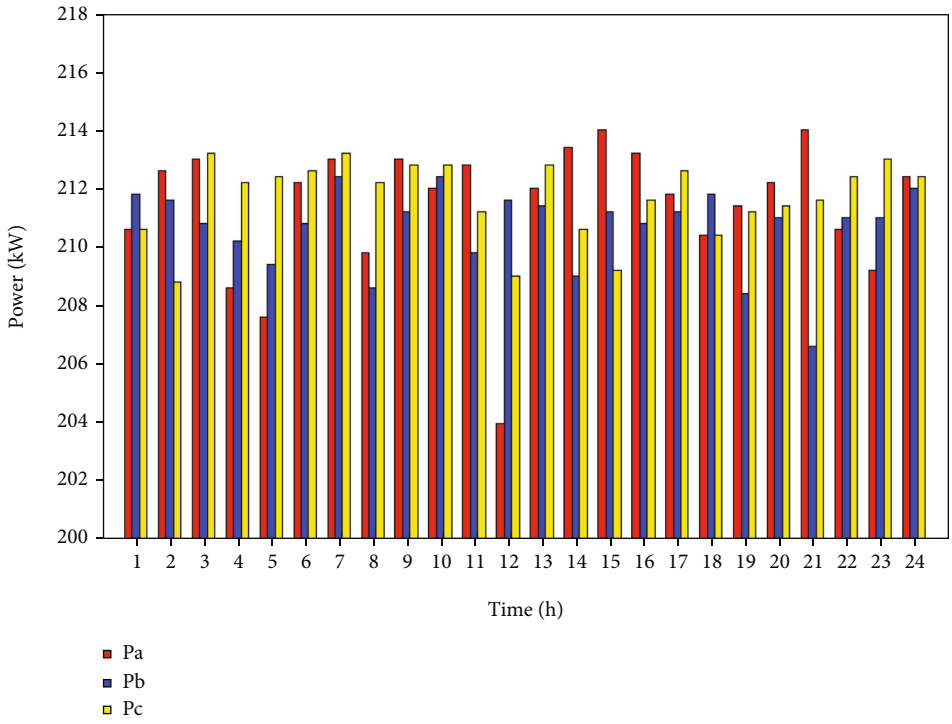

Figure 5: Active output power of the DG unit at Bus-12.

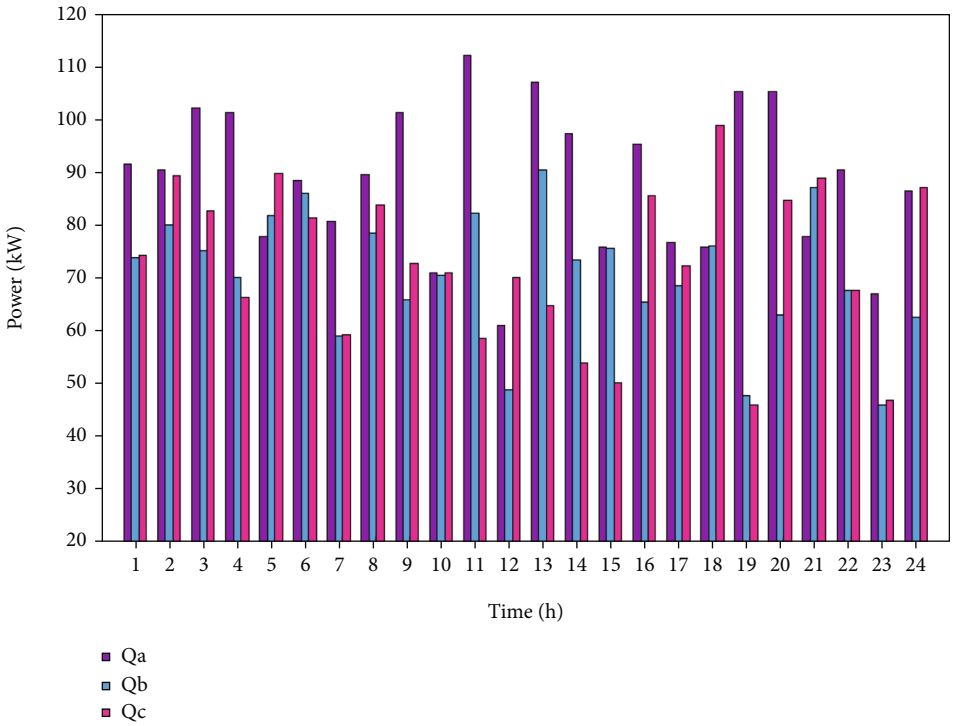

Figure 6: Reactive output power of the DG unit at Bus-12.

adopted to solve the optimal topology of the upper-level subsystem with the known switching states and DG outputs solved in the lower-level agent. Then, the optimal topology of the whole distribution system and the actual output power of all DG units are obtained based on real-time data within the current time window. At this point, the distribution reconfiguration is completed, and the DG units are in the optimal operating state, which will remain unchanged until the next time window when the scheduling plan for the next cycle is re-evaluated.

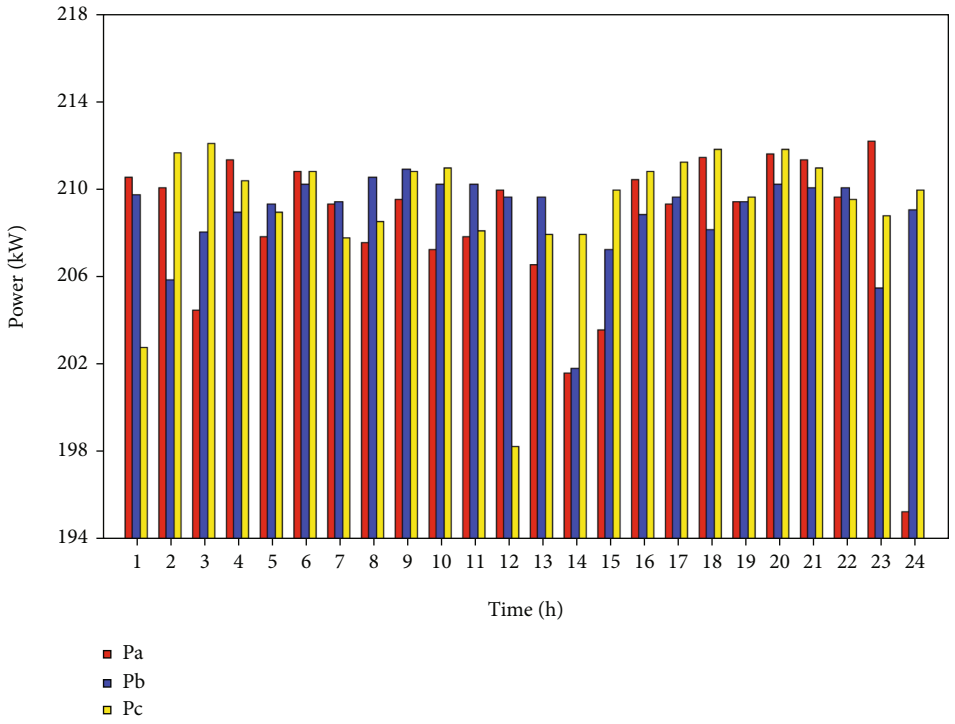

Figure 7: Active output power of the DG unit at Bus-13.

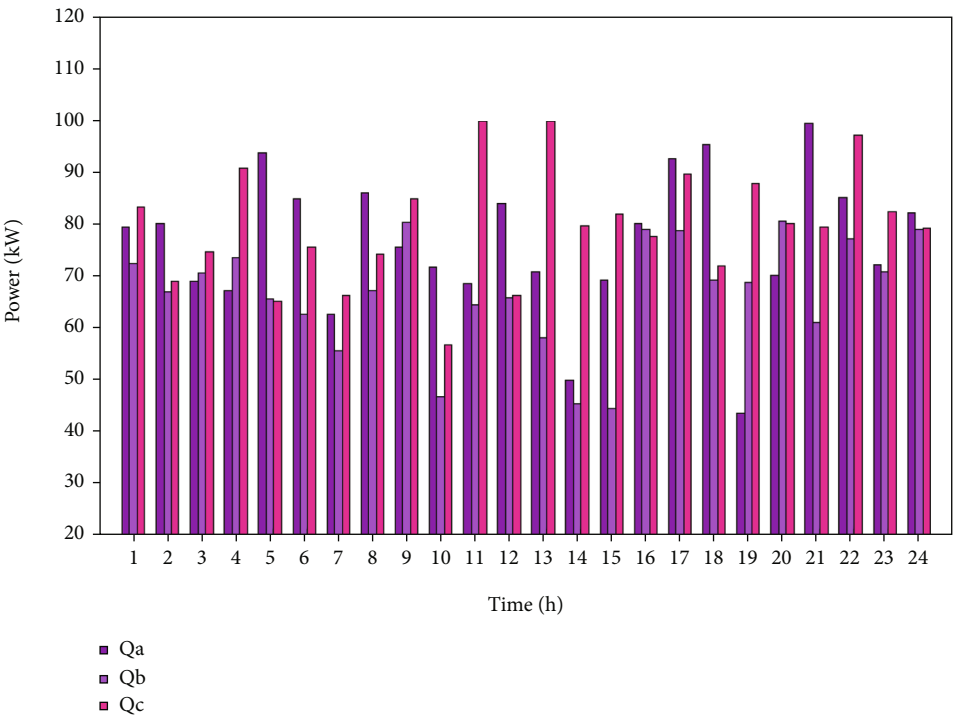

Figure 8: Reactive output power of the DG unit at Bus-13.

5. Algorithm Simulation

The simulated system of the distribution network used in this paper is a 25-node unbalanced system [18] with unbalanced line impedance and load distribution as shown in Figure 3.The system has three tie switches, 25, 26 and 27, respectively. Under normal operation, the interconnection switch is open. The initial three-phase power loss is 450.38 kW, and the minimum voltage is 0.93 pu.

In this paper, the load is modeled with a Gaussian mixture model (GMM) proposed in the literature [19], and the probability density function of the GMM is determined by

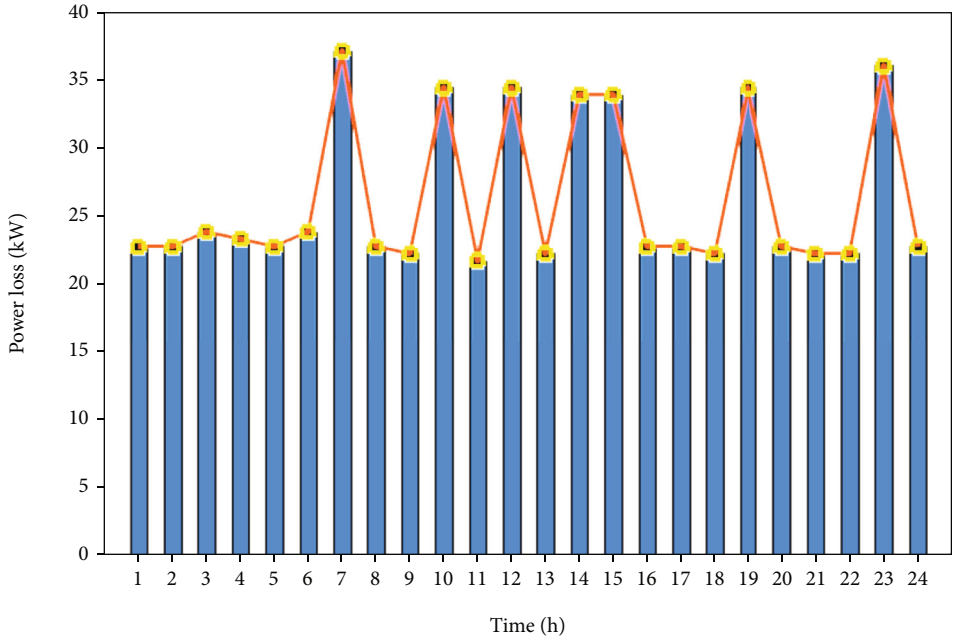

Figure 9: System power loss within 24 hours.

the following equation:

$$f(z) = \sum_{i=1}^{AM} w_i N(\mu_i, \sigma_i). \tag{31}$$

In the formula, AM is the number of components in the mixture model, μ_i is the mean, σ_i is the standard deviation, and w_i is the weight.

A GMM is applied randomly to each load. So the actual load power is obtained by multiplying the initial value by the unit value generated by the GMM. Monte Carlo simulations were performed, and the results showed that buses 12, 13, 11, 10, 15, 17, 14, and 9 were consistently the most sensitive 8 buses out of all 200 samples. To demonstrate the effectiveness of power loss reduction by installing DG units on the most sensitive buses, a system with 8 DG units on each of the 8 buses mentioned above is installed. After the DG unit locations are determined, the optimal capacity of each DG unit can be solved. Three scenarios are tested with a capacity limit of 500 kW/500kVA per phase DG, and the proposed Newton algorithm converges quickly after 5 to 20 iterations for different scenarios. The optimal capacities of DG units for the three scenarios are given in Table 2:

(1) Install a DG unit at the most sensitive bus 12

(2) Install a DG unit at bus 12 and 13, respectively

(3) Install a DG unit at bus 12, 13 and 11, respectively

Tests were conducted on several scenarios, and the results are shown in Table 2.

The results show that the optimal capacity of the DG units can be successfully solved while satisfying all system constraints. The integration of DG units helps to reduce power losses, increase voltage, and reduce voltage imbalance. The results of scenarios 2 and 3 are significantly better than those of scenario 1, indicating that the integration of multiple decentralized small-capacity DG units is more helpful than the integration of one large-capacity DG unit. Comparing the results from scenarios 2 and 3, the integration of two DG units already reduces the losses significantly, and adding a third DG unit does not help much. Therefore, the final decision was made to install two DG units at buses 12 and 13.

The operation period is set to 1 h, and the starting point is 0 : 00. 4 sets of 24-hour load curves are input to the system as real-time load data as shown in Figure 4.

The optimal switching scheme is shown in Table 3:

The following graphs give the actual output of the DG unit for 24 hours as shown in Figures 5–9.

6. Conclusion

A hierarchical decentralized distribution network reconfiguration method is proposed based on the characteristics of three-phase unbalanced distribution network reconfiguration. Network decomposition and multi-agent architecture are used to obtain the optimal reconfiguration scheme. In addition, although multiple agents are set up, the necessary information exchange between them is only the switching status of their subsystems, so the information transfer is low. The network reconfiguration algorithm has been applied in an unbalanced 25 node system. The simulation results show that the algorithm can reduce the power loss and the imbalance degree of the system.

Data Availability

Data sharing is not applicable to this article as no new data were created or analyzed in this study.

Conflicts of Interest

The author states that this article has no conflict of interest.

Acknowledgments

This work was supported by the Scientific research fund project of Education Department of Liaoning Province of China No. JL-2020.

References

[1] M. E. Baran and F. F. Wu, "Network reconfiguration in distribution systems for loss reduction and load balancing," *IEEE Power Engineering Review*, vol. 4, no. 2, pp. 101-102, 1989.

[2] M. W. Siti, D. V. Nicolae, A. A. Jimoh, and A. Ukil, "Reconfiguration and load balancing in the Lv and Mv distribution networks for optimal performance," *IEEE Transactions on Power Delivery*, vol. 22, no. 4, pp. 2534–2540, 2007.

[3] G. K. V. Raju and P. R. Bijwe, "An efficient algorithm for minimum loss reconfiguration of distribution system based on sensitivity and heuristics," *IEEE Transactions on Power Apparatus and Systems*, vol. 23, no. 3, pp. 1280–1287, 2008.

[4] F. V. Gomes, S. Carneiro, J. L. R. Pereira, M. P. Vinagre, P. A. N. Garcia, and L. R. D. Araujo, "A new distribution system reconfiguration approach using optimum power flow and sensitivity analysis for loss reduction," *IEEE Transactions on Power Apparatus and Systems*, vol. 21, no. 4, pp. 1616–1623, 2006.

[5] N. Gupta, A. Swarnkar, and K. R. Niazi, "Distribution network reconfiguration for power quality and reliability improvement using genetic algorithms," *International Journal of Electrical Power & Energy Systems*, vol. 54, pp. 664–671, 2014.

[6] M. A. Kashem, G. B. Jasmon, A. Mohamed, and M. Moghavvemi, "Artificial neural network approach to network reconfiguration for loss minimization in distribution networks," *International Journal of Electrical Power & Energy Systems*, vol. 20, no. 4, pp. 247–258, 1998.

[7] W. C. Wu and M. S. Tsai, "Application of enhanced integer coded particle swarm optimization for distribution system feeder reconfiguration," *IEEE Transactions on Power Apparatus and Systems*, vol. 26, no. 3, pp. 1591–1599, 2011.

[8] J. A. Taylor and F. S. Hover, "Convex models of distribution system reconfiguration," *IEEE Transactions on Power Apparatus and Systems*, vol. 27, no. 3, pp. 1407–1413, 2012.

[9] M. Lavorato, J. F. Franco, M. J. Rider, and R. Romero, "Imposing radiality constraints in distribution system optimization problems," *IEEE Transactions on Power Apparatus and Systems*, vol. 27, no. 1, pp. 172–180, 2012.

[10] J. C. Wang, H. D. Chiang, and G. R. Darling, "An efficient algorithm for real-time network reconfiguration in large scale unbalanced distribution systems," *IEEE Transactions on Power Apparatus and Systems*, vol. 11, no. 1, pp. 511–517, 1996.

[11] S. K. Goswami and S. K. Basu, "A new algorithm for the reconfiguration of distribution feeders for loss minimization," *IEEE Transactions on Power Delivery*, vol. 7, no. 3, pp. 1484–1491, 1992.

[12] B. Currie, C. Abbey, G. Ault et al., "Flexibility iskey in New York: new tools and operational solutions for managing distributed energy resources," *IEEE Power and Energy Magazine*, vol. 15, pp. 20–29, 2017.

[13] H. F. Zhai, M. Yang, B. Chen, and N. Kang, "Dynamic reconfiguration of three-phase unbalanced distribution networks considering unbalanced operation constraint of distributed generation," *International Journal of Electrical Power & Energy Systems*, vol. 99, pp. 1–10, 2018.

[14] Y. Haichuan, Z. Bide, and W. Haiying, "Distribution network dynamic reconfiguration method for improving distribution network's ability of accepting DG," *Power System Technology*, vol. 40, no. 5, pp. 1431–1436, 2016.

[15] X. Bai, Y. Mavrocostanti, D. Strickland et al., "Corrigendum: distribution network reconfiguration validation with uncertain loads - network configuration determination and application," *IET Generation, Transmission & Distribution*, vol. 11, no. 2, pp. 582–582, 2017.

[16] H. M. Ahmed, A. B. Eltantawy, and M. M. Salama, "A planning approach for the network configuration of AC-DC hybrid distribution systems," *IEEE Transactions on Smart Grid*, vol. 9, no. 3, pp. 2203–2213, 2018.

[17] X. Wang, Y. Ji, J. Wang, Y. Gao, and L. Qi, "Research on distribution network reconfiguration based on microgrid," *Journal of Ambient Intelligence and Humanized Computing*, vol. 11, no. 9, pp. 3607–3615, 2020.

[18] J. B. V. Subrahmanyam and C. Radhakrishna, "A simple method for feeder reconfiguration of balanced and unbalanced distribution systems for loss minimization," *Electric Power Components & Systems*, vol. 38, pp. 72–84, 2010.

[19] R. Singh, B. C. Pal, and R. A. Jabr, "Statistical representation of distribution system loads using Gaussian mixture model," *IEEE Transactions on Power Systems*, vol. 25, no. 1, pp. 29–37, 2010.